

OBSERVATIONS OF THE MOTION AND DISTRIBUTION OF THE IONIZED GAS IN THE CENTRAL PARSEC OF THE GALAXY. II.

J. H. LACY AND C. H. TOWNES

Department of Physics, University of California, Berkeley

T. R. GEBALLE

Mount Wilson and Las Campanas Observatories, Carnegie Institution of Washington

AND

D. J. HOLLENBACH

NASA Ames Research Center, Moffett Field, California

Received 1979 July 9; accepted 1980 April 16

ABSTRACT

Observations of infrared fine-structure line emission from compact clouds of ionized gas within Sgr A West are presented. These clouds have diameters of 0.1–0.5 pc, internal velocity dispersions $\sim 100 \text{ km s}^{-1}$ (FWHM), and line center velocities up to $\pm 260 \text{ km s}^{-1}$. Their masses are not accurately determined but are probably between 0.1 and $10 M_{\odot}$. They are ionized by radiation like that of stars of $T_{\text{eff}} \lesssim 35,000 \text{ K}$. The clouds are shown to have lifetimes $\sim 10^4 \text{ yr}$ and so must be generated and dissipated at a rate of a few per 10^3 yr . From analysis of the distribution of the velocities of the clouds, a most probable mass distribution is derived which includes a central pointlike mass of several $\times 10^6 M_{\odot}$ in addition to several $\times 10^6 M_{\odot}$ of stars within 1 pc of the center. However, the small number of clouds (14) makes the mass determination quite uncertain. A distributed mass of $\sim 10^7 M_{\odot}$ within the central parsec, with no central massive object, has a likelihood 1.4σ below that of the most probable distribution.

Subject headings: galaxies: Milky Way — galaxies: nuclei — infrared: sources

I. INTRODUCTION

Infrared fine-structure line emission of Ne II from the galactic center has been observed a number of times, with successively higher spatial and spectral resolution (Aitken, Jones, and Penman 1974; Wollman *et al.* 1976, 1977; Lacy *et al.* 1979). The study of infrared fine-structure emission from Sgr A West by Lacy *et al.* (hereafter Paper I) pointed out that there are compact clouds of ionized gas within Sgr A West, most of which are associated with $10 \mu\text{m}$ continuum sources. The measured velocities of these clouds appeared to be due to random motions in addition to rotation about an axis nearly perpendicular to the axis of the Galaxy. From these velocities, a mass of $\sim 8 \times 10^6 M_{\odot}$ within the central parsec was derived. Observations of Ne II and Ar III and a search for S IV and Ar V indicated that the degree of ionization in Sgr A West is unusually low in comparison to most other galactic H II regions.

Subsequent analysis of these observations has allowed more quantitative statements regarding the distribution of mass in the galactic center, the requirements on the ionizing radiation, and the nature of the compact ionized gas clouds. In this paper we first give a more complete presentation of the data, including a description of the gas clouds and the degree of ionization of the gas (§ II). This is followed by a discussion of the observations (§ III) in which we draw con-

clusions from the data regarding the distribution of mass, the lifetimes of the clouds, the gas density in the clouds, and the requirements on the spectrum of ionizing radiation. In this section we also show that there is dynamical evidence for a central massive object of a few times $10^6 M_{\odot}$ in addition to a comparable mass of stars in the central parsec, but that the number of clouds observed (14) does not provide an adequate statistical base to demonstrate convincingly the existence of a central pointlike mass. If present, this object would presumably be a black hole. If such a mass concentration is not present, the total star cluster mass within 1 pc radius would be approximately $1.2 \times 10^7 M_{\odot}$.

II. OBSERVATIONS

The data presented in this paper, a part of which were included in Paper I, were obtained using the 2.5 m du Pont telescope of Las Campanas Observatory during 1978 April and May. For the Ne II ($12.8 \mu\text{m}$) observations, the beam size was $3''.5$ (FWHM), and the spectral resolution corresponded to a Doppler width of 77 km s^{-1} . Beam positions were determined by offsetting from a nearby visible star whose coordinates were measured by offsetting from SAO stars to be $17^{\text{h}}42^{\text{m}}30^{\text{s}}.1 \pm 0^{\text{s}}.1$, $-28^{\circ}59'02'' \pm 1''$ (1950). (Becklin *et al.* 1978a place this star at $30^{\circ}0$, $01'.5$, and in 1979 we remeasured its position to be $29^{\circ}98 \pm 0^{\circ}04$,

$02^{\circ}8 \pm 0^{\circ}9$. The 1979 measurement would change all positions by $0^{\circ}12$ W, $0^{\circ}8$ S from those quoted in this paper.) The Ne II spectra from the central region of Sgr A West are displayed in Figure 1, arranged according to beam position. For each spectrum the central vertical line is at $v_{\text{LSR}} = 0$ and the horizontal line is at zero intensity. The offset of the baseline from zero intensity seen in most positions is due to continuum radiation. The data bars are approximately 2σ in height.

As was discussed in Paper I, the primary conclusion from these spectra is that the ionized gas is found in compact clouds, the velocities of which can be determined from the spectra. Except in the central region where the clouds overlap and can be separated only because of their different velocities, each cloud is associated with a peak in the distribution of $10\ \mu\text{m}$ continuum radiation. Conversely, each $10\ \mu\text{m}$ source has an associated gas cloud except for IRS 3 and IRS 7, neither of which has a spectrum like that of warm dust in an H II region. The one-to-one correspondence between ionized gas clouds and $10\ \mu\text{m}$ continuum sources indicates that it is unlikely that more clouds will be found, except possibly in the confused inner region or some distance from the center, where the infrared continuum is not yet completely mapped.

Figure 2a shows a map of the continuum emission at $12.8\ \mu\text{m}$, near the Ne II wavelength. Figures 2b–2f are maps of various velocity components of the line. These maps demonstrate most clearly the existence of separate ionized gas clouds and their coincidence with continuum emission peaks. In Figure 3, the velocities of the clouds are shown, superposed on the $10\ \mu\text{m}$ continuum map of Becklin *et al.* (1978a). As was pointed out in Paper I, positive and negative velocity clouds in the inner region (that shown in Fig. 1) can be separated by an axis approximately perpendicular to that of the Galaxy, whereas the more distant clouds follow galactic rotation more closely, with a NW–SE axis. However, considerable random motions are seen, and no simple disk pattern is evident.

The Ne II emission from the region surrounding that of Figure 1 has not been completely mapped. Several spectra from this region are shown in Figure 4. In the positions sampled, the Ne II intensity is approximately proportional to the $10\ \mu\text{m}$ continuum intensity from the map of Rieke, Telesco, and Harper (1978). This relation was assumed in the calculation of the total Ne II intensity, given in Table 1.

a) Cloud Description

A total of 14 compact clouds of ionized gas within a $1'$ (3 pc) diameter region at the galactic center have been identified from the data in this paper. These clouds are concentrated toward the center of the region, with roughly half of them found in the central $15''$. Measured and derived parameters related to these clouds are listed in Table 1. They may be summarized as follows:

1) The rms line-of-sight cloud velocity is $126 \pm 20\ \text{km s}^{-1}$, with the largest velocities found near the center.

2) The line-of-sight velocity variation (FWHM) within a cloud, after approximate correction for the instrumental resolution, is typically $100\ \text{km s}^{-1}$.

3) Cloud diameters are 0.1 – 0.5 pc, with the largest clouds found farthest from the center.

4) If the clouds were spheres of uniform density and the Ne⁺ abundance cosmic ($n_{\text{Ne}^+}/n_{\text{H}^+} = 0.8 \times 10^{-4}$), each cloud would contain 0.6 – $10\ M_{\odot}$ of ionized gas. If the clouds were very clumpy ($\langle n_e^2 \rangle^{1/2} / \langle n_e \rangle \gtrsim 100$), their masses would be as small as $\sim 0.1\ M_{\odot}$.

5) Each cloud must absorb $\sim 10^{49}$ Lyman continuum photons s^{-1} , again assuming $n_{\text{He}^+}/n_{\text{H}^+} = 0.8 \times 10^{-4}$. About 2×10^{50} ionizing photons s^{-1} must be absorbed by all of the gas observed in the central 3 pc.

b) Ionic Abundances

Observations of the central region of Sgr A West at the frequencies of infrared emission lines of H, Ne, S, and Ar and of the radio continuum emission have been made by several groups. Measurements centered on IRS 1 for these various species are listed in Table 2. To allow comparison of observations with different beam sizes, each ionic flux has been divided by the Ne II flux from the same area, estimated from the spectra in Figure 1. The ionic abundances relative to Ne⁺ are given in column (7) of Table 2. These figures were derived assuming no collisional de-excitation of the excited fine-structure states, i.e., $n_e \ll n_c$, where n_e is the electron density in the regions which produce the dominant amount of line emission, and n_c (col. [9]) is the critical electron density for collisional de-excitation (Petrosian 1970). To correct for the effect of collisional de-excitation, each ionic density, n_i , should be multiplied by $1 + n_e/n_c$. In using the ratios of other fluxes to those of Ne II, all ions are assumed to have the same spatial distribution as Ne⁺.

The primary uncertainty in the abundance ratio calculations is in the correction for interstellar extinction. The extinction values assumed here were taken from Figure 1 of Becklin *et al.* (1978b) for $\lambda \geq 7\ \mu\text{m}$ and from their Table 1 for $\lambda < 7\ \mu\text{m}$. Their discussion indicates that the extinction near $10\ \mu\text{m}$ is uncertain by about $\pm 50\%$, primarily as a result of the uncertainty in the depth of the silicate feature. A 50% increase in the depth of the silicate absorption would increase $n_{\text{S}^{+3}}/n_{\text{Ne}^+}$ and $n_{\text{Ar}^{+2}}/n_{\text{Ne}^+}$ by a factor of 2.5 and decrease $n_{\text{Ar}^+}/n_{\text{Ne}^+}$ by a factor of 1.4. The ratio $n_{\text{Ar}^{+2}}/n_{\text{Ar}^+}$ would increase by a factor of 3.5.

The possibility that some of the fine-structure levels are collisionally saturated leads to additional uncertainties in the ionic abundance ratios. If collisional de-excitation is negligible, the ratio of the abundance of argon in the observed ionization states to that of Ne⁺ is about 1.8 times the cosmic Ar/Ne abundance ratio, and the ratio $n_{\text{Ar}^{+2}}/n_{\text{Ar}^+}$ is ~ 0.1 . Because of the higher density required to thermalize the Ar II fine-structure

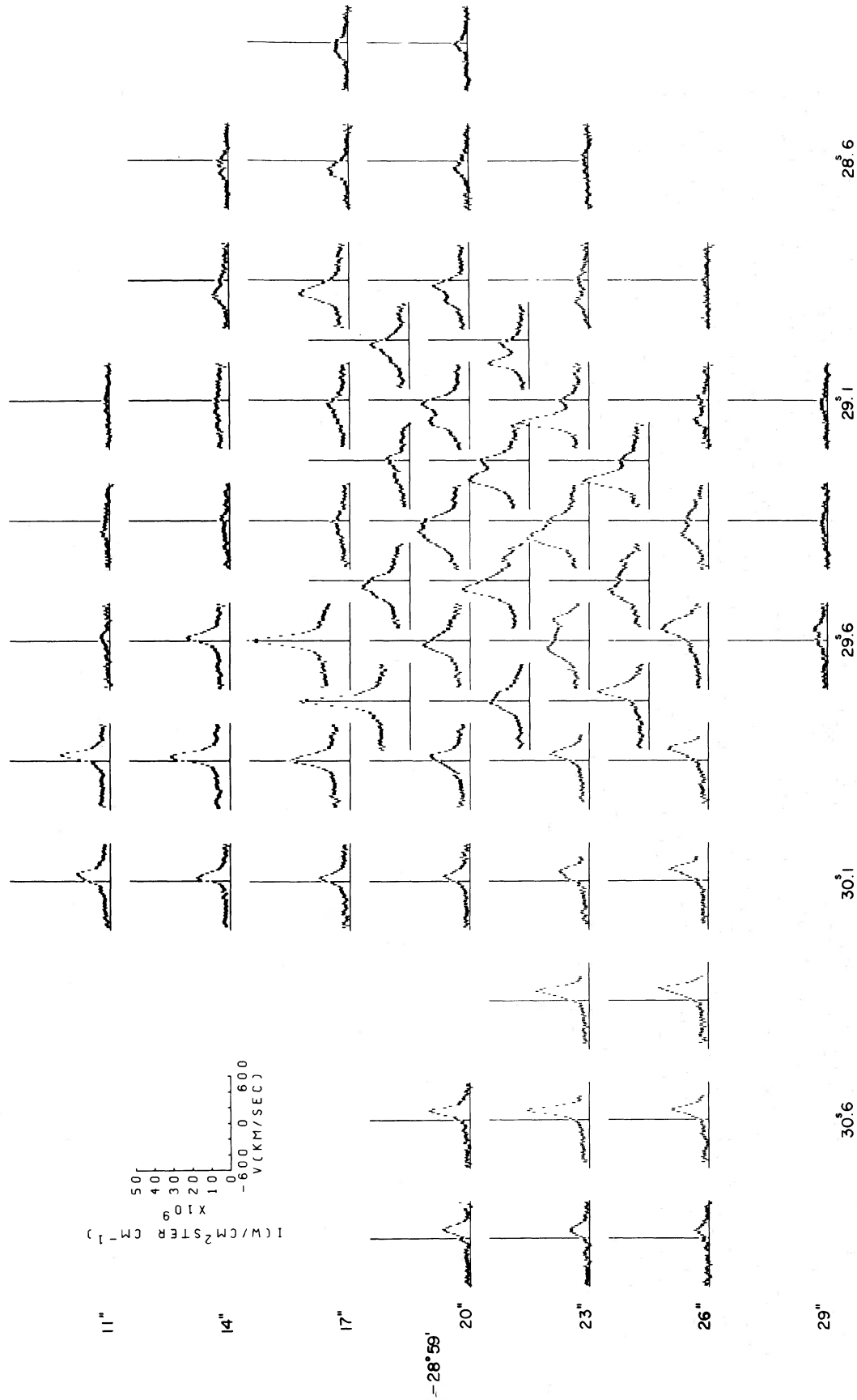


FIG. 1.—Ne II (12.8 μ m) spectra from the central region of the Galaxy. The coordinates on the left and bottom label the beam positions relative to 17^h42^m, -28°59' (1950). The central vertical axis of each spectrum is at $v_{LSR} = 0$, and the horizontal axis is at zero intensity. Intensity and velocity scales are given on the upper left axes. Intensities are not corrected for interstellar extinction. Beam size is 3".5 (FWHM), velocity resolution is 77 km s⁻¹ (FWHM).

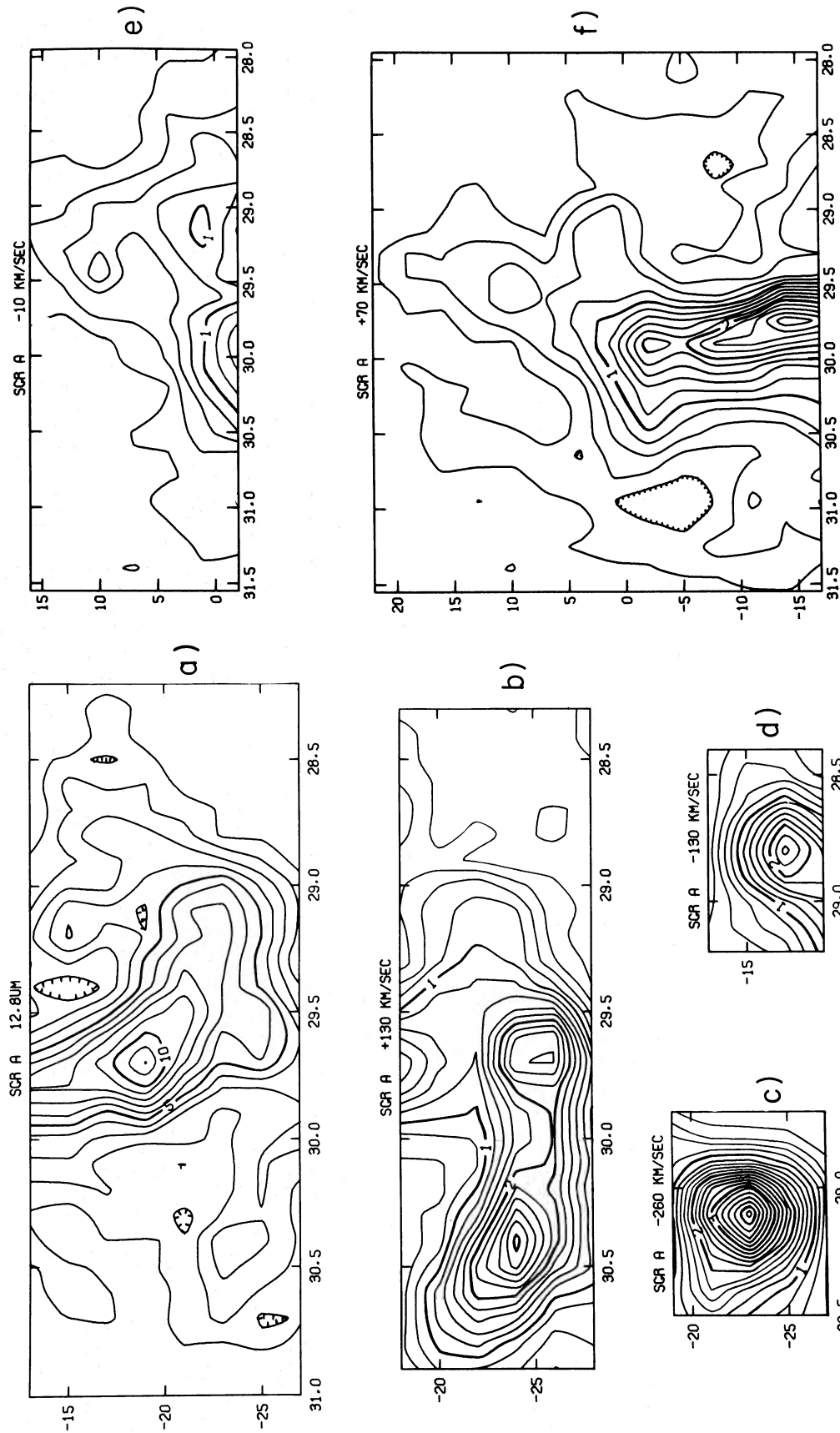


FIG. 2.—(a) Contour map of 12.8 μm continuum emission. Contours are labeled in units of 10^{-9} W ($\text{cm}^2 \text{sr cm}^{-1}$) $^{-1}$. Beam size is $3''.5$. Coordinates are relative to $17^{\text{h}}42^{\text{m}}, -28^{\circ}59'$ (1950). (b)–(f)—Contour maps of Ne II emission at various velocities, showing localization of gas of a given velocity. Contours are labeled in units of 10^{-8} W ($\text{cm}^2 \text{sr cm}^{-1}$) $^{-1}$.

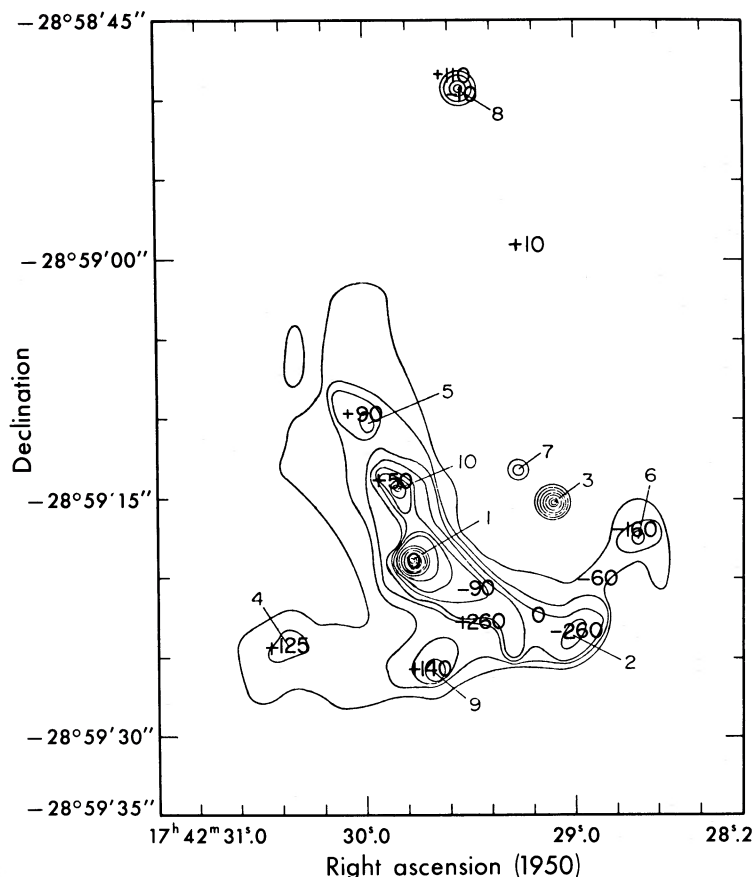


FIG. 3.—Velocities of ionized gas clouds (*bold face numbers*) superposed on 10 μm continuum map of Becklin *et al.* (1978a)

levels, any correction for collisional de-excitation will increase the derived value of $n_{\text{Ar}^{+2}}/n_{\text{Ar}^{+}}$ toward 0.3 and decrease $(n_{\text{Ar}^{+}} + n_{\text{Ar}^{+2}})/n_{\text{Ne}^{+}}$ toward the cosmic Ar/Ne ratio. At an electron density of $n_e = 3 \times 10^5$, approximately twice the cosmic abundances of neon and argon would be required. In light of the probable increased stellar processing of material near the galactic center, these abundances seem plausible and are perhaps more likely than an overabundance of only argon. Assuming cosmic S/Ne and $n_e \ll 10^5 \text{ cm}^{-3}$, the limit on S IV indicates that $n_{\text{S}^{+3}}/n_{\text{S}} \leq 0.02$, and for $n_e \gg 3 \times 10^5$ that $n_{\text{S}^{+3}}/n_{\text{S}} \leq 0.08$, where n_{S} refers to the sum of all ionization states of sulfur. The value of n_e in the regions which dominate the emission is discussed in § III. Errors in pointing and in the corrections for different beam sizes contribute smaller uncertainties in the abundance determinations than those discussed above.

III. DISCUSSION

a) Position of the Galactic Center

There is no distinguishing feature in the Ne II spectra which clearly identifies a particular position as the dynamical center of the Galaxy. However, a region $\sim 5''$ in radius, centered at $17^{\text{h}}42^{\text{m}}29^{\text{s}}.5$, $-28^{\circ}59'22''$,

includes both the two highest velocity components and the densest concentration of gas clouds. In addition, any axis which separates positive from negative velocity clouds within the central region (that contained within the lowest infrared continuum contour of Fig. 3) passes near this position. For the purpose of calculations in this paper we will consider this position to be the galactic center. It is difficult to specify the uncertainty in this determination, but it seems very unlikely that the center could lie outside the $5''$ circle mentioned here.

It has been proposed that a $2.2 \mu\text{m}$ source, IRS 16 (Becklin and Neugebauer 1975), and the compact non-thermal radio source (Balick and Brown 1974) are located at the center of the Galaxy. IRS 16 is at $17^{\text{h}}42^{\text{m}}29^{\text{s}}.3$, $-28^{\circ}59'20''$, $\sim 3''$ NW of our preferred position of the center, and the radio source is at $17^{\text{h}}42^{\text{m}}29^{\text{s}}.3$, $-28^{\circ}59'18''$, $\sim 5''$ NW of our center. The uncertainty in comparisons of the radio and infrared positions is $\sim 3''$. The uncertainty in comparisons of the various infrared positions is less, $\sim 1''$, since the same guide star was used for all measurements and several sources are seen at 2, 10, and $12.8 \mu\text{m}$. The position of IRS 16 is consistent with our determination of the position of the center within the uncertainties, although it is somewhat off the axis

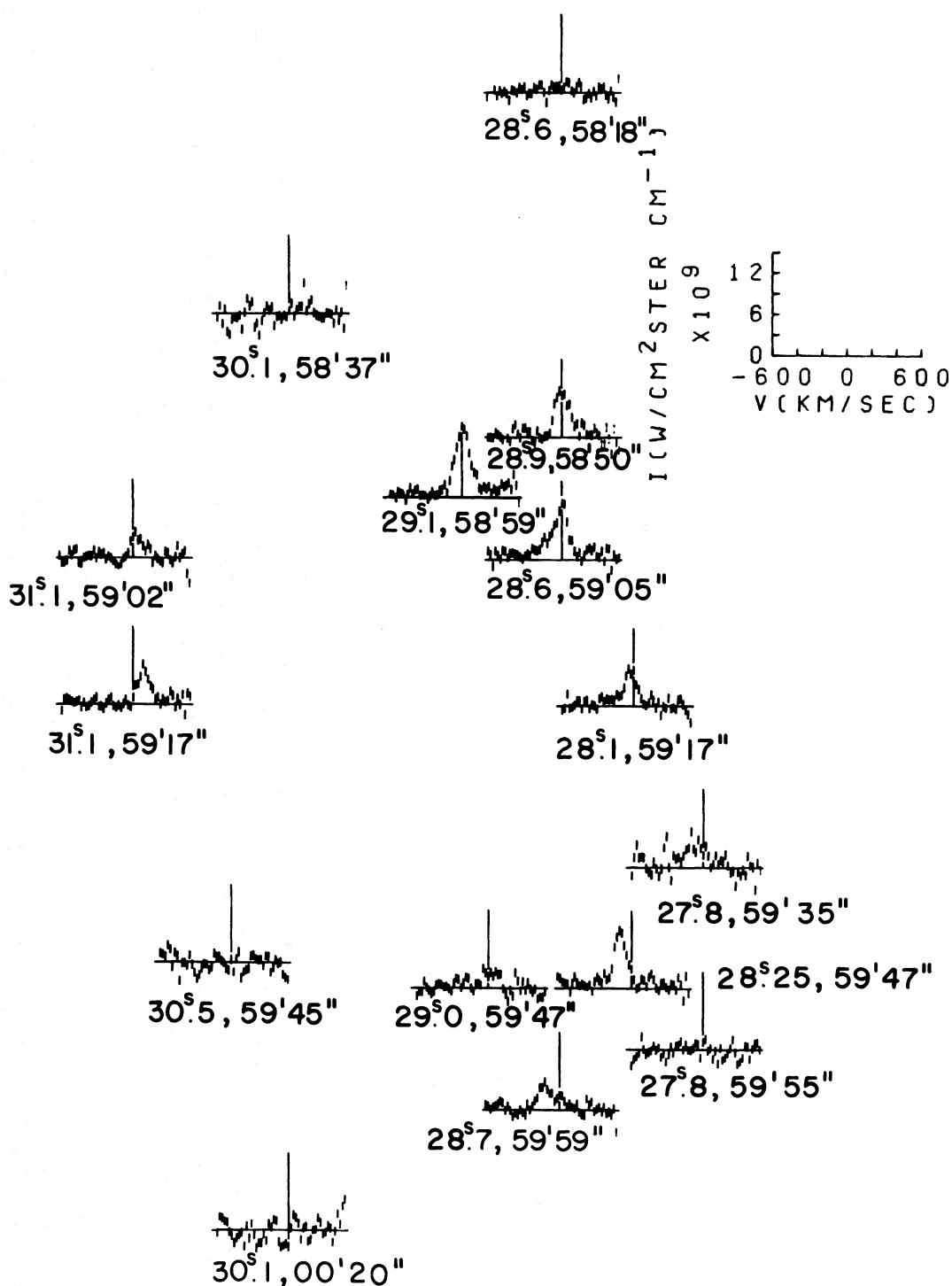


FIG. 4.—Ne II spectra from positions surrounding the region shown in Fig. 1. Coordinates are given below each spectrum.

of rotation. The distance from the Ne II center to the compact radio source is somewhat larger, although also less certain. IRS 1, which, like IRS 16, is a bright $2.2 \mu\text{m}$ emitter, lies on the axis of rotation and is coincident with a Ne II cloud with $v_{\text{LSR}} \approx 0$. It too must be considered a candidate for the location of

the galactic center, although it is displaced from the center of concentration of gas clouds.

b) Mass Distribution

The velocities of the ionized clouds in Sgr A were used in Paper I to derive a mass of $8 \times 10^6 M_{\odot}$ within

TABLE 1
CLOUD PARAMETERS

IRS Number	R.A. (17 ^h 42 ^m)	Decl. (-28°59')	<i>r</i> (pc)	<i>D</i> (pc)	<i>v</i> _{LSR} (km s ⁻¹)	Δv (km s ⁻¹)	EM _{peak} (10 ⁶ cm ⁻⁶ pc)	∫EM (10 ⁶ cm ⁻⁶ pc ³)	<i>M</i> _{nom} (M _⊙)	<i>M</i> _{min} (M _⊙)	Φ _{Lyc} (10 ⁴⁸ s ⁻¹)	Age (10 ³ yr)
	29:50	23'	0.05	0.10	+260	100	1.0
	29:50	21	0.05	0.25	-90	180	1.4
9	29:65	25	0.18	0.25	+140	130	17	...	3.1	0.14	11	1.9
	29:20	22	0.20	0.15	0	100	20	1.4	1.5
1	29:70	18	0.24	0.10	0	70	24	1.0	0.67	0.10	8	1.4
2	29:10	22.5	0.26	0.25	-260	100	16	1.4	3.1	0.14	11	2.5
	29:00	20	0.34	0.20	-60	120	1.7
10	29:75	14	0.43	0.20	+50	70	14	2.9
6	28:80	17	0.52	0.25	-160	140	19	1.3	3.0	0.12	11	1.8
4	30:40	24	0.59	0.35	+125	80	16	2.3	6.7	0.22	18	4.4
5	29:80	10	0.68	~0.30	+80	80	4.4
	29:10	00	1.13	0.25	+10	70	3.6	7.1
8	29:50	58:50 ^a	1.60	0.45	-10 ^a	50	8.8	2.0	9.1	0.18	16	7.5

NOTE.—*r*, Projected distance from 17^h42^m29^s.5, -28°59'22"; distance from Sun to galactic center assumed = 10 kpc. *D*, Cloud diameter, approximately corrected for 3'.5 resolution. *v*_{LSR}, Line center radial velocity. Δv , FWHM line-of-sight velocity variation within each cloud after approximate correction for 77 km s⁻¹ resolution. EM_{peak}, Peak emission measure, measured with a 3'.5 beam. ∫EM, Emission measure integrated over each cloud. *M*_{nom}, Cloud mass assuming constant density within a sphere of a radius *r*. *M*_{min}, Cloud mass assuming sufficient clumping so that *n*_e >> *n*_c. Φ_{Lyc}, Lyman continuum flux required to ionize each cloud. Age, *D*/Δ*v*. EM_{peak}, ∫EM, *M*_{nom}, *M*_{min}, and Φ_{Lyc} assume *n*_{Ne⁺}/*n*_{H⁺} = 0.8 × 10⁻⁴.

^a Two velocity components are seen here and many indicate the presence of two overlapping clouds.

TABLE 2
IONIC ABUNDANCES IN SAGITTARIUS A WEST FOR VARIOUS FIELDS OF VIEW CENTERED ON IRS 1

Line (λ) (1)	F_{obs} ($10^{-18} \text{ W cm}^{-2}$) (2)	θ (arcsec) (3)	A (mag) (4)	F_{corr} ($10^{-18} \text{ W cm}^{-2}$) (5)	$\int n_i n_e dV$ ($\text{cm}^{-6} \text{ pc}^3$) (6)	n_i/n_{Ne} (7)	γ_{cosmic} (8)	n_e (cm^{-3}) (9)	Reference (10)
Bz (4.0 μm)	5.7 ^a	17	1.2	17	6.9×10^6	1.2×10^4	10^4	...	Soifer <i>et al.</i> 1976
	2.6 ± 0.2	8	...	8	3.2×10^6	1.9×10^4	Bally <i>et al.</i> 1979
By (2.2 μm)	1.1 ± 0.1	32	2.7	13	1.6×10^7	1.0×10^4	Neugebauer <i>et al.</i> 1978
Ne II (12.8 μm)	6.2 ± 1	4	1.1	17	60	1	0.83	3.6×10^5	This paper
	17 ± 4	8	...	46	170	
	50 ± 10	16	...	138	510	
	80 ± 16	22	...	210	810	
	500	total ^b	...	1380	5100	
Ar II (7.0 μm)	64 ± 12	28	0.7	122	140	0.13	0.063	1×10^6	Willner <i>et al.</i> 1979
Ar III (9.0 μm)	0.3 ± 0.15	8	3.0	5	2.3	0.014	...	3×10^5	This paper
Ar V (13.1 μm)	<0.4	4	1.0	<1	<0.6	<0.01	...	8×10^4	This paper
S IV (10.5 μm)	<0.1	8	3.1	<2	<0.7	<0.004	0.16	9×10^4	This paper
5 GHz continuum	$26 \pm 4 \text{ Jy}$	total ^c	2.8×10^7	5.5×10^3	10^4	...	Ekers <i>et al.</i> 1975

NOTE.— F_{obs} : Measured flux. θ : Beam size centered on IRS 1. A : Extinction correction from Becklin *et al.* 1978b (magnitudes). F_{corr} : Flux corrected for extinction ($10^{-18} \text{ W cm}^{-2}$). $\int n_i n_e dV$: Derived ionic volume emission measure. For fine-structure lines the formulae of Petrosian 1970 and collision strengths of Kruuger and Czyzak 1970, Brocklehurst 1972, and Seaton 1975 were used. The hydrogen line strengths were calculated from Pengelly 1964. n_i/n_{Ne} : Ratio of ionic abundance to Ne^+ in same beam size interpolated from fluxes listed. These are obtained by summing measured fluxes from Fig. 1. γ_{cosmic} : Cosmic atomic abundance, $H = 10$ (Allen 1973). n_e : Critical electron density for collisional de-excitation (Petrosian 1970).

^a Uncertain due to nearby terrestrial atmospheric absorption.

^b Total Ne II flux estimated by assuming $J_{\text{Ne II}}/I_{6-13 \mu\text{m}} = \text{constant}$ and using continuum map of Rieke *et al.* 1978.

^c Total 5 GHz flux measured within an approximately $30''$ radius.

the central parsec of the Galaxy. Although the small number of objects observed (14) makes any detailed analysis of the mass distribution uncertain, the fact that the highest velocity clouds are found closest to the center suggests that the gravitational potential results from a more centrally concentrated mass distribution that is expected in an isothermal star cluster.

An additional uncertainty occurs in the determination of the mass distribution because the objects whose velocities are measured are gas clouds rather than stars. Gas and dust can be acted on by nongravitational forces, such as radiation and gas pressure. If these forces were dominant, the cloud velocities could not be used to measure the gravitational potential. As a first approximation, we will assume that the cloud orbits are determined predominantly by gravity. The force of radiation can be estimated from the luminosity of each cloud (assuming that the radiation emitted equals that absorbed) and is typically small compared to gravity. However, interactions between the clouds must certainly be important when they collide and may affect the observed velocity distribution. A further difficulty arises because the cloud velocities are not known to have an isotropic distribution.

We calculate here the mass distributions using two different assumptions, that the clouds move in randomly oriented circular orbits or that the clouds are formed from a population of stars in hydrostatic equilibrium and so have velocities and positions distributed like those of stars. In the first case, the mass within a distance r of the center is given by $M(r) = v_{\text{orb}}^2(r)r/G$. If to correct for projection effects, it is assumed that $v_{\text{orb}}^2(r) = 3\sigma_v^2(r)$, where σ_v is the observed rms line-of-sight velocity dispersion,

$$M(r) = \frac{3r}{G} \sigma_v^2(r). \quad (\text{III.1})$$

A group of stars bound in the gravitational potential of a mass distribution, $M(r)$, and with a spatial distribution, $n(r)$, must satisfy the equation of hydrostatic equilibrium,

$$\frac{d}{dr} [n(r)\sigma_v^2(r)] = -\frac{GM(r)}{r^2} n(r). \quad (\text{III.2})$$

We will assume that the clouds are generated either from single stars or by stellar collisions. If we take $\sigma_v(r)$ and $n(r)$ of the clouds as measures of σ_v and n of some uniform group of stars from which they were formed (or in the case of clouds formed by collisions between stars of masses m_1 and m_2 , σ_v and n apply to a group of stars with masses $m_1 + m_2$), equation (III.2) can be solved for $M(r)$. For $0.2 \text{ pc} < r < 1.5 \text{ pc}$, the observed distribution of clouds fits a power law, $n(r) \propto r^{-\beta}$, where $\beta = 3.5 \pm 0.5$, as illustrated in Figure 5. With a power law distribution equation (III.2) gives

$$M(r) = \frac{1}{G} \left[-r^2 \frac{d}{dr} \sigma_v^2(r) + \beta r \sigma_v^2(r) \right]. \quad (\text{III.3})$$

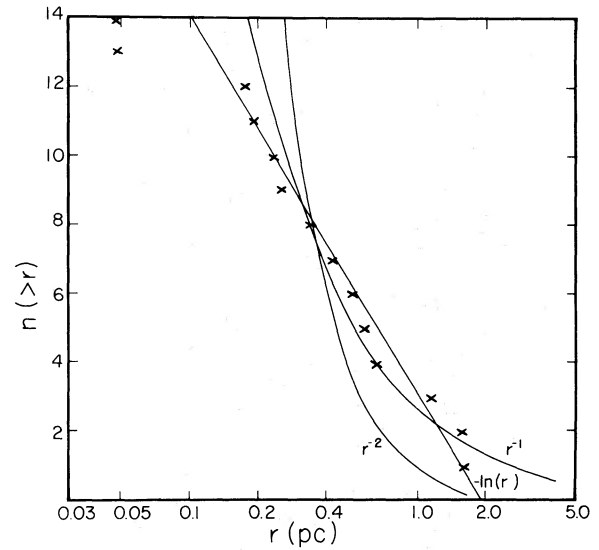


FIG. 5.—Number of clouds observed beyond a distance r from the galactic center versus r . The notations $n(>r) \propto -\ln r$, r^{-1} , r^{-2} correspond to $n(r) \propto r^{-3}$, r^{-4} , r^{-5} . Except for $r < 0.1 \text{ pc}$, the observed distribution of clouds is fitted equally well by $n(r) \propto r^{-3}$ or r^{-4} .

Both equations (III.1) and (III.3) give $M(r) \propto r$ if $\sigma_v(r)$ is a constant. This is the expected mass distribution outside the core of an isothermal star cluster. In the core, orbital velocities decrease toward the center, and the density distribution of a group of stars would not follow a power law. If we approximate the mass distribution of a cluster containing a central massive object by $M(r) = M_0 + M_1 r$, equations (III.1) and (III.3) each require $\sigma_v^2(r) = \sigma_0^2 + b/r$, where for the case of circular orbits,

$$M_0 = 3b/G \quad \text{and} \quad M_1 = 3\sigma_0^2/G. \quad (\text{III.4})$$

If the clouds provide a measure of an equilibrium stellar distribution,

$$M_0 = (\beta + 1)b/G \quad \text{and} \quad M_1 = \beta\sigma_0^2/G. \quad (\text{III.5})$$

In the case of a star cluster containing a massive central black hole, M_0 includes both the black hole mass and the mass associated with enhanced stellar density due to perturbation of the stellar cluster distribution by the black hole.

What is actually observed is $\sigma_v(r_\perp)$, the average of $\sigma_v(r)$ along a line of sight at a projected distance r_\perp from the center. This quantity also has the form $\sigma_v^2(r_\perp) = \sigma_0^2 + b'/r_\perp$, where for $n(r) \propto r^{-\beta}$ and $3 < \beta < 4$, $0.79b < b' < 0.85b$. The parameters σ_0^2 and b' were determined by fitting the cloud velocities in Table 2 to a Gaussian velocity distribution with a mean velocity, $\bar{v} = 0$, and a standard deviation, $\sigma_v^2(r_\perp) = \sigma_0^2 + b'/r_\perp$. The maximum likelihood method was used. The most probable values were determined to be $\sigma_0^2 = 4320 \text{ km}^2 \text{ s}^{-2}$ and $b' = 2930 \text{ km}^2 \text{ s}^{-2} \text{ pc}$.

Because the uncertainties in σ_0^2 and b' are correlated, we display the relative probabilities of these parameters (the likelihood), $p(\sigma_0^2, b')$, as a contour

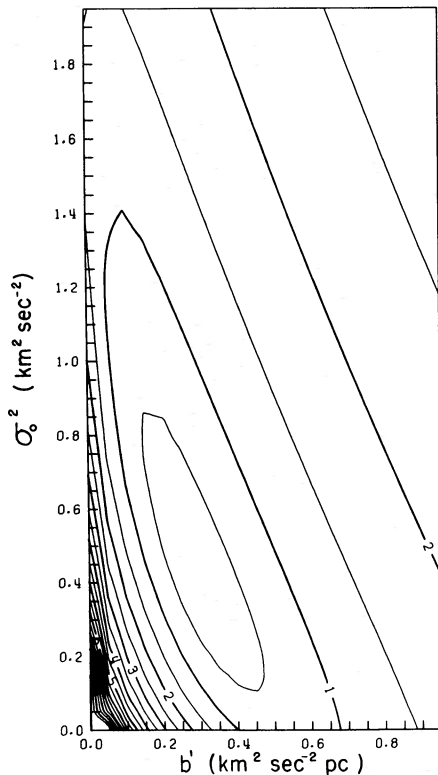


FIG. 6.—Contour plot showing relative probability of various values of σ_0^2 and b' , where the observed mean square velocity is $\sigma_v^2(r_\perp) = \sigma_0^2 + b'/r_\perp$. σ_0^2 is proportional to the distributed mass, and b' to the central pointlike mass. Contours are labeled in units of one standard deviation; axes, in units of $10^4 \text{ km}^2 \text{ s}^{-2} \text{ pc}$ and $10^4 \text{ km}^2 \text{ s}^{-2}$.

plot in Figure 6. The quantity plotted is $z = [-2 \ln(p/p_{\max})]^{1/2}$ so that $p(\sigma_0^2, b') = \exp(-z^2/2)$, and z represents the number of standard deviations from the most likely values. This figure shows that the most likely value of b' if $\sigma_0^2 = 0$ (no distributed mass) has a probability of ~ 0.7 standard deviations below the peak. The most likely value of σ_0^2 if $b' = 0$ (no central mass) is $1.6 \times 10^4 \pm 0.4 \times 10^4 \text{ km}^2 \text{ s}^{-2}$, the mean squared cloud velocity. This point is ~ 1.4 standard deviations below the peak. The large uncertainty in the determination of σ_0^2 and b' is not the result of any error in the measured velocities but rather is due to the uncertainty in determining the variation of velocity dispersion with radius from a small sample.

For the circular orbit assumption we obtain $M(r) = (3.0 \times 10^6 r_{\text{pc}} + 2.5 \times 10^6) M_\odot$, and for the assumption of an equilibrium distribution of cloud positions and velocities, $M(r) = (3.5 \times 10^6 r_{\text{pc}} + 3.7 \times 10^6) M_\odot$, where $r_{\text{pc}} = r/1 \text{ pc}$. In either case, the uncertainties in the parameters are comparable to their values. If it is assumed that no point mass is present, we obtain $M(r) = (1.1 \pm 0.3) \times 10^7 r_{\text{pc}} M_\odot$ and $M(r) = (1.3 \pm 0.4) \times 10^7 r_{\text{pc}} M_\odot$ for the two cases.

Two velocity components are associated with the last cloud in Table 1 (IRS 8). Since one of the

velocity components ($+110 \text{ km s}^{-1}$) appears to be a continuation of the ridge extending north from IRS 1, only the other (-10 km s^{-1}) was included in the above calculations. However, the calculations were also made including both components. The best fit mass distribution was then $M(r) = (4.5 \times 10^6 r_{\text{pc}} + 2.0 \times 10^6) M_\odot$ for the circular orbit assumption and $(5.2 \times 10^6 r_{\text{pc}} + 3.0 \times 10^6) M_\odot$ for the equilibrium distribution assumption. The likelihood of a mass distribution with no central object remained $\sim 1.4 \sigma$ below the most probable.

The higher gas velocities toward the center of Sgr A have also been noted by Rodriguez and Chaisson (1979). They point out that the radio recombination lines which have been observed with 1:3–4' beam widths are only about one-half as broad as the Ne II line from the central $20''$ (1 pc). They conclude that the radio measurements are dominated by an extended relatively low-density halo surrounding the region of most intense Ne II emission and that a central pointlike mass of $\sim 5 \times 10^6 M_\odot$ could account for the variation of velocity dispersion with radius. If σ_0 , the velocity dispersion beyond the region dominated by a possible central massive object, were assumed to be determined accurately by the recombination line observations, a more statistically significant determination of the variation of σ_v with r than that calculated here could be made. We choose not to make this assumption because part of the radio emission comes from a few individual clouds, and so has a statistical uncertainty not apparent in a large beam measurement, and part from diffuse gas of uncertain location and dynamics. There is appreciable diffuse ionized gas at relatively low velocity, but uncertainties in its relation to the galactic center and in effects on the motion of any part of it due to its origin or due to interaction with the other parts of this material make the velocity distribution difficult to interpret. These uncertainties are much less for the compact clouds.

c) Cloud Lifetimes

It was suggested in Paper I that each cloud could be bound to a massive object, such as a dense cluster of stars, and so could have a lifetime substantially longer than the free expansion time of $\lesssim 10^4 \text{ yr}$. A mass of $1-2 \times 10^5 M_\odot$ would be required to bind each cloud. There are several problems with this suggestion. If the massive objects were star clusters, they would be disrupted on a time scale comparable to that for collisions between gas clouds, $\sim 2 \times 10^4 \text{ yr}$, unless they were much smaller than the clouds. Condensed objects, such as black holes or extremely compact star clusters, would not be disrupted but would scatter from each other and as a result evaporate from the core in less than 10^6 yr (see Saslaw 1973) unless they could lose energy sufficiently rapidly through dynamical friction with field stars. In this case, they would spiral toward the center.

A second conceivable means of preventing expan-

sion of the clouds is confinement by the pressure of a hot external medium. However, the internal velocities of the clouds are not much less than their relative velocities, so that for allowable temperatures of the intercloud medium, a density approaching that within the clouds would be required in order to bind them. The temperature of such a medium is restricted to $T \gtrsim 10^6$ K, in order that the intercloud gas density be sufficiently low to allow cloud motion, and to $T \lesssim 10^7$ K in order that the medium not evaporate. For $T \lesssim 3 \times 10^6$ K the medium will produce $\sim 10^7 L_\odot$ of ~ 100 eV photons which will photoionize Ne and Ar in the clouds to much higher stages of ionization than are observed. For $T \gtrsim 3 \times 10^6$ K, the medium will produce far more 1–3 keV X-rays (approximately 10^{38} ergs s^{-1}) than are observed (10^{35} ergs s^{-1} , Giacconi 1979). There does appear to be an extended halo in which the clouds are embedded, but its temperature is that of an H II region, not $\sim 10^7$ K as would be required to contain the clouds.

It therefore appears that the clouds cannot be bound against their internal velocity dispersions and that the observed line widths must represent expansion. An age can then be determined for each cloud by dividing its diameter by its velocity of expansion, with the assumption that the expansion velocity has been present since the cloud's creation. These ages, listed in Table 1 for these clouds whose sizes have been measured, are in the range $1-8 \times 10^3$ yr, with the oldest clouds found farthest from the center. The high end of this age range is comparable to the time between cloud collisions, possibly indicating that collisions finally destroy the clouds. Assuming that the observed numbers and ages of clouds are typical, clouds must form at a rate of $\sim 2 \times 10^{-3}$ yr $^{-1}$.

Even if the clouds are not bound against their internal velocity dispersions, they might be regenerated if turbulence which produces clumping on the scale of the cloud dimensions could be fed into the gas to replace that lost by expansion of the clouds. The motions of stars through the gas clouds fail to maintain such turbulence both because the rate of energy transfer is too small and because the turbulence produced would be on a much smaller scale than that observed. A very inhomogeneous gravitational field resulting from star clusters or compact massive objects might be able to provide the proper energy input. However, we have already argued that interactions between such objects would either disrupt them or eject them from the central region. In the absence of any regeneration mechanism, the gas in the clouds which dissipate must be removed from the interstellar medium of the galactic center.

d) Densities and Masses of the Clouds

The Ne II measurements do not allow an accurate determination of the masses of the ionized gas clouds because the fine-structure line fluxes depend quadratically on the gas density for densities below the critical density for collisional de-excitation, n_c . Two

estimates of the cloud masses are given in columns (10) and (11) of Table 1. The "nominal" mass, M_{nom} , is derived assuming that each cloud is a uniform sphere of gas, with no small-scale clumping. A lower limit to the cloud masses, M_{min} , is derived assuming sufficient clumping that $n_e \gg n_c$ in the regions which dominate the Ne II emission. In both cases $n_{\text{Ne}^+}/n_{\text{H}^+} = 0.8 \times 10^{-4}$ is assumed. A measurement of the clumpiness of the clouds would be required to determine their masses and the effects of collisional saturation on the ionic abundance ratios.

The gas density in clumps in an H II region is normally measured from the ratio of two lines of an ion which has a critical density for collisional saturation near the gas density. No such pair of lines has yet been reported for Sgr A West. Ar III (9.0 μm , 21.8 μm) with $n_c \sim 10^5 \text{ cm}^{-3}$, S III (18.7 μm , 33.6 μm) with $n_c \sim 3 \times 10^3 \text{ cm}^{-3}$, or possibly O III (51.7 μm , 88.2 μm) with $n_c \sim 10^3 \text{ cm}^{-3}$ could serve the purpose. Alternatively, N II (121.7 μm) with $n_c \sim 10^2 \text{ cm}^{-2}$ could be used as a direct measure of the cloud masses since N^+ is probably the dominant ionization state of N and the fine-structure levels of N^+ should be well thermalized. If $n_{\text{Ar}^+}/n_{\text{N}^+}$ is assumed to equal cosmic Ar/N, the line ratio Ar II/N II could also be used to measure n_e . Any of these measurements would have to be made with a sufficiently small beam so that emission from the clouds would dominate that from more diffuse material. A 20" beam would be desirable but at present is not possible for the longer wavelength lines.

Although no determination of the clumpiness or filling factor has yet been made, the covering factor (projected filling factor) can be estimated from radio continuum and Brackett line observations. The emission measure through the line emitting clumps, determined from the turnover frequency of the radio continuum, can be compared to the spatially averaged emission measure, determined from short-wavelength, optically thin, emission. The free-free optical depth is given by $\tau_{\text{ff}} = 3.3 \times 10^{-7} \nu_9^{-2.1} T_4^{-0.65} \text{ EM}$, where $\nu_9 = \nu/(10^9 \text{ Hz})$ and $T_4 = T_e/10^4 \text{ K}$. Several relevant observations are listed in Table 3. The dependence of emission measure on beam size can be approximately corrected for by assuming that $\text{EM} \propto \theta^{-1}$ as is observed in Ne II. While comparison of results of different observers is somewhat uncertain because of calibration and beam-size problems, the fact that no strong dependence on frequency is seen in the emission measures derived assuming optically thin emission indicates that τ_{ff} is not large for $\nu \geq 2.7 \text{ GHz}$. Balick and Sanders (1974) state that the 8.1 GHz brightness is about twice that at 2.7 GHz, which would indicate $\tau_{\text{ff}}(2.7 \text{ GHz}) \sim 1$, and $\text{EM} \sim 2 \times 10^7 \text{ cm}^{-6} \text{ pc}$. This is equal to the emission measure averaged over the 8" beam of Bally, Joyce, and Scoville (1979), indicating that the covering factor once the clouds are resolved is of order 1. Hence, if the clouds are clumpy, the clumps are sufficiently numerous to cover most of each cloud.

The entire range of cloud masses given in Table 2,

TABLE 3
HYDROGEN LINE AND FREE-FREE CONTINUUM INTENSITIES

Spectral Region	θ (arcsec)	I ($\text{W cm}^{-2} \text{sr}^{-1}$ or K)	EM ($10^6 \text{ cm}^{-6} \text{ pc}$)	Reference
B α	17	3.3×10^{-9}	10	Soifer <i>et al.</i> 1976
	8	6.9×10^{-9}	20	Bally <i>et al.</i> 1979
B γ	32	7.0×10^{-10}	6	Neugebauer <i>et al.</i> 1978
23 GHz	5×21	36 K	9	Wright 1979
8.1 GHz	6×21	$\sim 600 \text{ K}^a$	15	Balick and Sanders 1974
5 GHz	6.3×34	720 K	7	Ekers <i>et al.</i> 1975
2.7 GHz	6×21	2700 K	7	Balick and Sanders 1974

NOTE.— θ , Beam size. I , Intensity. EM, Emission measure.

^a Approximately twice the 2.7 GHz intensity.

M_{min} to M_{nom} , must at present be considered possible. Even larger masses of ionized gas could be present in low-density wings on the clouds or in intercloud material.

e) Ionization Mechanisms

Although the possibility of collisional saturation of fine-structure levels and errors in the extinction correction make conclusions about relative ionic abundances rather uncertain, it appears that the ionization state of Sgr A is significantly lower than that of most other galactic H II regions. If $n_e \lesssim 10^5 \text{ cm}^{-3}$ and if the extinction corrections in Table 1 are correct, $n_{\text{Ar}^{+2}}/n_{\text{Ar}} \sim 0.1$ and $n_{\text{S}^{+3}}/n_{\text{S}} \sim 0.02$. Even with the considerable uncertainties, definite upper limits of $n_{\text{Ar}^{+2}}/n_{\text{Ar}} < 0.5$ and $n_{\text{S}^{+3}}/n_{\text{S}} < 0.2$ can be set. In contrast, Ar^{+2} is the dominant ionization state of Ar in most other H II regions that have been studied, and S^{+3} is often abundant.

Several mechanisms might be considered to help explain the observed distribution of ionic abundances: (1) The gas could be ionized by shocks. (2) Each cloud could be ionized by an embedded star with a spectral distribution appropriate for producing the low ionization state. (3) The gas could be ionized by stars or other sources lying outside the clouds. (4) A source of harder radiation might be allowed in option 2 or 3 if the spectrum could be softened by dust absorption. (5) A very hard ultraviolet source might leave enough neutral H and He to charge exchange with multiply-ionized species. These possible mechanisms are discussed in the remainder of this section.

(1) Shock waves ionize gas by electronic and atomic collisions in the hot postshock gas, as well as by photoionization by Lyman continuum photons radiated by the cooling and recombining postshock ions. The observations require a process which will ionize Ne and Ar (ionization thresholds at 21.6 and 15.8 eV) without ionizing too much Ar^+ (threshold at 27.6 eV). Collisions dominate the ionization of the rare gases for shock velocities $v_s \lesssim 100 \text{ km s}^{-1}$ (Shull and McKee 1979), but the resulting surface brightness of the Ne II (12.8 μm) line from such a shock front is at least three

orders of magnitude below that observed. Shocks with $v_s \gtrsim 100 \text{ km s}^{-1}$ photoionize the rare gases. However, in the range $100 \text{ km s}^{-1} < v_s < 200 \text{ km s}^{-1}$ (Shull and McKee 1979; Raymond 1979) and probably in the range $200 \text{ km s}^{-1} < v_s < 500 \text{ km s}^{-1}$, shocks radiate large fluxes of He II $\text{L}\alpha$ at 40.8 eV, which produces larger abundances of Ar^{+2} and S^{+3} than are observed. Shocks with speeds $v_s > 500 \text{ km s}^{-1}$ and which produce the required ionizing luminosity would emit more X-radiation than is observed from Sgr A West ($\lesssim 10^2 L_{\odot} \text{ keV}^{-1}$ at 3 keV; see, e.g., Bradt, Doxsey, and Jernigan 1979). More generally, energetic arguments rule out ionization by shocks; the total ionizing luminosity required by the observations would mean the injection of $12v_2^{-2} M_{\odot} \text{ yr}^{-1}$ of material at velocity $v_2 \equiv v/100 \text{ km s}^{-1}$. We know of no reasonable source or sink for such a mass flow.

(2) and (3) The total ionizing luminosity which is absorbed by the gas in the central 3 pc can be calculated from the observed emission to be $\Phi_{\text{Lyc}} \approx 2 \times 10^{50}$ Lyman continuum photons per second. However, unless the sources of ionizing radiation are embedded in the clouds, the emitted luminosity must be larger than this, since not all of the radiation will be intercepted by the clouds. If the ionizing radiation is emitted by a central source or group of sources, a lower limit to the emitted luminosity can be calculated by dividing the luminosity absorbed by a cloud by the fraction of the solid angle from the center which it subtends. Such an estimate, using the most distant bright source, IRS 8, gives $\Phi_{50} = \Phi_{\text{Lyc}}/10^{50} \text{ s}^{-1} \gtrsim 20$. The sizes and luminosities of nearer clouds require $\Phi_{50} \gtrsim 8$. Since IRS 8 might have additional local sources of ionizing radiation, $\Phi_{50} = 8$ is used below. A similar ionizing luminosity would have to be emitted by a distribution of sources not associated with individual clouds.

If each cloud is ionized by an embedded star, the required spectral types of the ionizing stars can be determined from model nebula calculations. The calculations of Balick and Sneden (1976) indicate that a $T_{\text{eff}} \leq 35,000 \text{ K}$ star will ionize a nebula to the observed degree. A single O8 I star or several O8 III stars could provide the ionizing luminosity required by a typical

cloud. No O7 stars could be present in the clouds without ionizing them to a higher ionization state than that which is observed.

In order to estimate the ionic abundances in a gas cloud ionized by radiation incident from outside, without making a detailed radiative transfer calculation, we assume that the gas in the He II zone sees the unattenuated ionizing radiation, whereas no photons of $h\nu > 24.6$ eV are present in the He I zone. In the He II zone, the fractional ionic abundances can then be calculated from equations of ionization-recombination equilibrium. Since recombination rates per ion scale as n_e and the ionization rates scale as $F_{\text{Lyc}} = \Phi_{\text{Lyc}}/(4\pi r^2)$, the ionization stage of a species depends on $\Phi_{\text{Lyc}} r^{-2} n_e^{-1}$, where r is the distance to the source of ionizing radiation. Therefore, we have plotted, in Figure 7, $x(m)/x_m$ versus $\Phi_{50} r_{\text{pc}}^{-2} n_4^{-1}$, where $x(m)$ is the fractional abundance of a specific ionization stage of species m , x_m is the total fractional abundance of that species, $\Phi_{50} = \Phi_{\text{Lyc}}/10^{50}$ Lyman continuum photons s^{-1} , $r_{\text{pc}} = r/(1 \text{ pc})$, and $n_4 = n_e/10^4 \text{ cm}^{-3}$. Three values of the effective temperature $T_4 = T_{\text{eff}}/10^4 \text{ K}$ of the source are displayed corresponding to continuum spectra from early type stars of temperatures $T_{\text{eff}} = 35,000 \text{ K}$, $40,000 \text{ K}$, and $50,000 \text{ K}$,

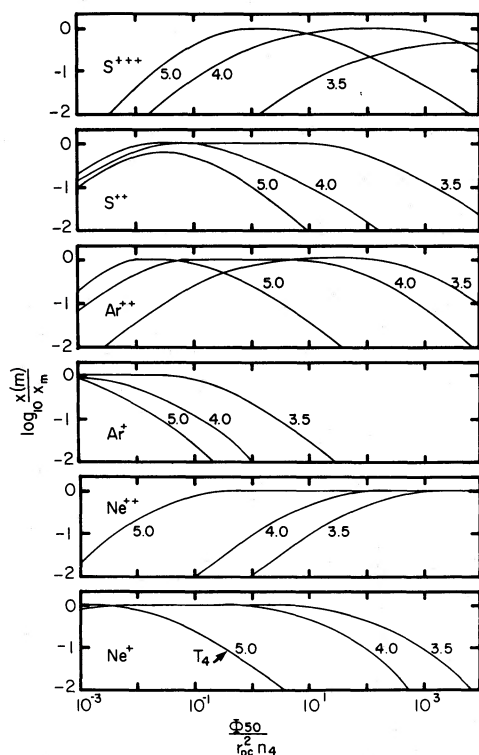


FIG. 7.—The fractional abundance of a particular ionic stage of an element $x(m)$ is plotted against the “ionizing power” $\Phi_{50} r_{\text{pc}}^{-2} n_4^{-1}$ of an unattenuated source, where Φ_{50} = ionizing photons per second in units of 10^{50} s^{-1} , r_{pc} = distance to ionizing source in pc, and n_4 = gas proton density in units of 10^4 cm^{-3} . Plots are made with three effective source temperatures $T_4 = T_{\text{eff}}/10^4 \text{ K} = 3.5, 4.0, \text{ and } 5.0$.

$\log g = 5$, and solar metal content (Kurucz 1970; Balick and Sneden 1976). Lower gravity or lower metal content tends to make these stars appear hotter, but these effects are small compared with the effect of temperature in determining the ionization stages of Ar, Ne, and S (cf. Balick and Sneden 1976). We have taken recombination coefficients from Aldrovandi and Péquignot (1973) for Ne and S and have calculated recombination coefficients for Ar from the prescription of Silk and Brown (1971). Photoionization cross sections have been taken from Osterbrock (1974) for Ne, from Chapman and Henry (1972) for Ar, and from Chapman and Henry (1971) for S.

In the case of a single central source of ionizing radiation, the cloud closest to the source places the strongest constraint on the ionizing spectrum. Taking $\Phi_{50} = 8$, a cloud at $r_{\text{pc}} = 0.2$ sees a flux of $\Phi_{50}/r_{\text{pc}}^2 = 200$. From Figure 7 it is then apparent for $T_{\text{eff}} \gtrsim 35,000 \text{ K}$ that no realistic value of n_e could allow argon to be singly ionized in the He II zone. The observed abundance ratio limit, $n_{\text{Ar}^+}/n_{\text{Ar}} < 0.5$, therefore requires that helium ionizing photons penetrate less than halfway through the innermost cloud. The helium ionizing luminosity required to ionize helium in one of the inner clouds is $\Phi_{\text{Hec}} \approx 6 \times 10^{48} \text{ s}^{-1}$. Consequently a central source of ionizing radiation must have $\Phi_{\text{Hec}}/\Phi_{\text{Lyc}} \lesssim 7.5 \times 10^{-3}$ to ionize hydrogen in one of the outer clouds while ionizing less than half of the helium in an inner cloud. An effective temperature $\lesssim 31,000 \text{ K}$ is required to produce this ratio of $\Phi_{\text{Hec}}/\Phi_{\text{Lyc}}$ (Kurucz 1979).

If the ionizing radiation comes from sources distributed uniformly throughout the region in which the clouds are found, each cloud will see essentially the same ionizing flux. The flux required to ionize the brightest cloud is $F_{\text{Lyc}} = 1.8 \times 10^{50} \text{ s}^{-1} \text{ pc}^{-2}$. Although the required density to allow singly ionized argon to exist is lower than in the case of a central source, lack of penetration of helium ionizing photons is still required to explain the observations. The flux of helium-ionizing photons which would only half penetrate a typical cloud is $F_{\text{Hec}} = 4 \times 10^{48} \text{ s}^{-1} \text{ pc}^{-2}$, requiring $\Phi_{\text{Hec}}/\Phi_{\text{Lyc}} < 0.022$. A $T_{\text{eff}} \leq 35,000 \text{ K}$ star would provide such a ratio.

(4) Chaisson, Lichten, and Rodriguez (1978) discuss the effect of absorption by grains on the ionization of Sgr B2. They conclude that grains with reasonable properties can reduce the volume of the He II Strömgren sphere to one-half that of the H II sphere by selective absorption of He ionizing radiation. To do this, the grain absorptivity at 500 \AA must be ~ 3 times higher than that at 900 \AA , and a substantial fraction of the ionizing radiation must be absorbed by grains. This effect may help to explain observed ionic abundances in Sgr A, but it appears unlikely that a large fraction of the ionizing radiation can be absorbed by grains since the $2\text{--}20 \text{ \mu m}$ luminosities of the individual clouds ($1\text{--}2 \times 10^5 L_{\odot}$, Becklin *et al.* 1978a) can be explained by absorption of trapped L α radiation with little additional energy input.

(5) Charge-exchange is also an unlikely mechanism for producing the observed low state of ionization. This mechanism requires a relatively high neutral fraction, ~ 0.01 , for H or He since charge exchange rate coefficients are approximately 100 to 1000 times larger than electronic recombination rate coefficients (Dalgarno and Butler 1978). In order to produce high neutral fractions, we require hard photons (since photoionization cross sections $\propto \nu^{-3}$) and high densities (since recombination rates $\propto n^2$). The results of Dalgarno and Butler (1978) suggest that Ar^{+2} may undergo a rapid charge exchange (rate coefficient $\sim 10^{-9} \text{ cm}^3 \text{ s}^{-1}$) with He, but not with H. Using reasonable values for photoionization, recombination, and charge rates, we find that a source producing 10^{50} photons per second of 0.3 keV energy results in a neutral fraction of $n_{\text{He}^+}/n_{\text{He}^{+2}} > 0.01$ at a distance of 1 pc and hence a relative abundance $n_{\text{Ar}^{+2}}/n_{\text{Ar}^{+}} < 0.3$ if $n \gtrsim 10^4 \text{ cm}^{-3}$. There are two major problems with this charge exchange mechanism, however. The first is that the results of Butler, Bender, and Dalgarno (1979) imply that there is no fast charge exchange process for Ne^{+2} . The second is that the photon source must peak around 0.3 keV ($\sim 3 \times 10^{40} \text{ ergs s}^{-1}$ luminosity in this region), but fall rapidly at higher energies (since $L \lesssim 1 \times 10^{35} \text{ ergs s}^{-1}$ for $1 \text{ keV} < h\nu < 3 \text{ keV}$ is observed, Giacconi 1979) and lower energies ($L \lesssim 10^{37} \text{ ergs s}^{-1}$ for the 13.6 eV–50 eV band since H and He must be ionized by the hard photons). We can propose no likely model for such a source.

The above discussion indicates that a source of relatively soft ionizing radiation is required to explain the observed ionic abundances. If the ionizing radiation comes from stars distributed throughout the central parsec, these stars must have effective temperatures $T_{\text{eff}} \lesssim 35,000 \text{ K}$. If the source or sources of ionizing radiation are concentrated at the center, $T_{\text{eff}} \gtrsim 31,000 \text{ K}$ is required. A collection of $T_{\text{eff}} = 35,000 \text{ K}$ stars with an ionizing luminosity of $\Phi_{50} = 8$ would have a bolometric luminosity of $L = 2.8 \times 10^7 L_{\odot}$. If $T_{\text{eff}} = 31,000 \text{ K}$, $L = 8.8 \times 10^7 L_{\odot}$. In either case, much of the stellar luminosity must escape from the central few parsecs of the Galaxy to avoid a conflict with the observed infrared emission from warm dust.

IV. CONCLUSIONS

We now summarize the conclusions which have been drawn from the observations.

1. *Mass distribution.* The most likely mass distribution derived from the cloud velocities consists of a central pointlike mass of $\sim 3 \times 10^6 M_{\odot}$ in addition to a distributed mass (assuming $\rho \sim r^{-2}$) of $\sim 3 \times 10^6 M_{\odot}$ within 1 pc of the center. The uncertainties in both masses are correlated and are about equal to their values, so that a mass distribution with no central pointlike mass cannot be ruled out. If no central massive object is present, the distributed mass within 1 pc is $(1.2 \pm 0.4) \times 10^7 M_{\odot}$.

2. *Cloud generation.* Gas clouds of $0.1\text{--}10 M_{\odot}$ and with internal velocity dispersions of $\sim 100 \text{ km s}^{-1}$ (FWHM) are being created at a rate of a few per 10^3 yr . The large uncertainty in the cloud masses results from the unknown amount of clumping of the gas.

3. *Ionization.* About 2×10^{50} Lyman continuum photons per second must be absorbed by the gas within 1.5 pc of the center of the Galaxy to account for its ionization. If the sources of this radiation lie outside the clouds, a total ionizing luminosity $\Phi_{\text{Lyc}} \sim 10^{51} \text{ s}^{-1}$ must be emitted. The spectral distribution of the radiation must be like that of stars of $T_{\text{eff}} \lesssim 35,000 \text{ K}$ if the radiation comes from a distribution of sources, whereas T_{eff} must be $\lesssim 31,000 \text{ K}$ if a central source is dominant.

4. *Gas sink.* A gas sink which accepts gas at a rate equal to that required for cloud production must be present.

Models which might explain these conclusions will be discussed in a subsequent paper (Lacy, Townes, and Hollenbach, in preparation).

We wish to thank the staff of Las Campanas Observatory for their hospitality and considerable assistance. F. Baas made important contributions to the design and construction of the spectrometer and participated in earlier observations. We are grateful for the generous advice and encouragement given by Prof. J. Oort. Professor C. F. McKee has made valuable suggestions on analysis of these results, and Professor E. Scott and Dr. D. W. Peterson provided advice on statistical problems. This work was supported in part by NASA grant 05-003-272 and NSF grant AST 78-24453. D. J. Hollenbach was supported by the Space Sciences Laboratory, U.C. Berkeley, NASA Core funds, and by an NRC Senior Associateship.

REFERENCES

- Aitken, D. K., Jones, B., and Penman, J. M. 1974, *M.N.R.A.S.*, **169**, 35.
 Aldrovandi, S. M. V., and Péquignot, D. 1973, *Astr. Ap.*, **25**, 137.
 Allen, C. W. 1973, *Astrophysical Quantities* (3d ed.; London: Athlone Press).
 Balick, B., and Brown, R. L. 1974, *Ap. J.*, **194**, 265.
 Balick, B., and Sanders, R. H. 1974, *Ap. J.*, **191**, 325.
 Balick, B., and Sneden, C. 1976, *Ap. J.*, **208**, 336.
 Bally, J., Joyce, R. R., and Scoville, N. Z. 1979, *Ap. J.*, **229**, 917.
 Becklin, E. E., Matthews, K., Neugebauer, G., and Willner, S. P. 1978a, *Ap. J.*, **219**, 121.
 ———. 1978b, *Ap. J.*, **220**, 831.
 Becklin, E. E., and Neugebauer, G. 1975, *Ap. J. (Letters)*, **200**, L71.
 Bradt, H. V., Doxsey, R. E., and Jernigan, J. G. 1979, *Adv. in Space Exploration*, **3**, 1.
 Brocklehurst, M. 1972, *M.N.R.A.S.*, **160**, 19P.
 Butler, S. E., Bender, C. F., and Dalgarno, A. 1979, *Ap. J. (Letters)*, **230**, L59.

- Chaisson, E. J., Lichten, S. M., and Rodriguez, L. F. 1978, *Ap. J.*, **221**, 810.
- Chapman, R. D., and Henry, R. J. W. 1971, *Ap. J.*, **168**, 169.
- . 1972, *Ap. J.*, **173**, 243.
- Dalgarno, A., and Butler, S. E. 1978, *Comments Atom. Molec. Phys.*, **7**, 129.
- Ekers, R. D., Gross, W. M., Schwartz, V. J., Downes, D., and Rogstad, D. H. 1975, *Astr. Ap.*, **43**, 159.
- Giacconi, R. 1979, private communication.
- Krueger, T. K., and Czyzak, S. J. 1970, *Proc. R. Soc. London, A* **318**, 531.
- Kurucz, R. L. 1970, *Smithsonian Ap. Obs. Spec. Rept.*, No. 309.
- . 1979, *Ap. J. Suppl.*, **40**, 1.
- Lacy, J. H., Baas, F., Townes, C. H., and Geballe, T. R. 1979, *Ap. J. (Letters)*, **227**, L17 (Paper 1).
- Neugebauer, G., Becklin, E. E., Matthews, K., and Wynn-Williams, C. G. 1978, *Ap. J.*, **220**, 149.
- Osterbrock, D. E. 1974, *Astrophysics of Gaseous Nebulae* (San Francisco: Freeman).
- Pengelly, R. M. 1964, *M.N.R.A.S.*, **127**, 145.
- Petrosian, V. 1970, *Ap. J.*, **159**, 833.
- Raymond, J. C. 1979, *Ap. J. Suppl.*, **39**, 1.
- Rieke, G. H., Telesco, C. M., and Harper, D. A. 1978, *Ap. J.*, **220**, 556.
- Rodriguez, L. F., and Chaisson, E. J. 1979, *Ap. J.*, **228**, 734.
- Saslaw, W. C. 1973, *Pub. A.S.P.*, **85**, 5.
- Seaton, M. J. 1975, *M.N.R.A.S.*, **170**, 475.
- Shull, J. M., and McKee, C. F. 1979, *Ap. J.*, **227**, 131.
- Silk, J., and Brown, R. L. 1971, *Ap. J.*, **163**, 495.
- Soifer, B. T., Russell, R. W., and Merrill, K. M. 1976, *Ap. J. (Letters)*, **207**, L83.
- Willner, S. P., Russell, R. W., Puetter, R. C., Soifer, B. T., and Harvey, P. M. 1979, *Ap. J. (Letters)*, **229**, L65.
- Wollman, E. R., Geballe, T. R., Lacy, J. H., Townes, C. H., and Rank, D. M. 1976, *Ap. J. (Letters)*, **205**, L5.
- . 1977, *Ap. J. (Letters)*, **218**, L103.
- Wright, M. 1979, private communication.

T. R. GEBALLE: Mount Wilson and Las Campanas Observatories, 813 Santa Barbara St., Pasadena, CA 91101

D. J. HOLLENBACH: NASA Ames Research Center, Mail Stop 245-6, Moffett Field, CA 94035

J. H. LACY: California Institute of Technology, Downs Laboratory of Physics, 320-47, 1201 E. California Blvd., Pasadena, CA 91125

C. H. TOWNES: University of California, Department of Physics, Berkeley, CA 94720